Appl. Phys. B (2016) 122:177
DOI 10.1007/s00340-016-6453-5

Applied Physics B
Lasers and Optics

Experimental long-term survey of mid-infrared supercontinuum source based on As_2S_3 suspended-core fibers

O. Mouawad[1] · S. Kedenburg[2] · T. Steinle[2] · A. Steinmann[2] · B. Kibler[1] · F. Désévédavy[1] · G. Gadret[1] · J-C Jules[1] · H. Giessen[2] · F. Smektala[1]

Received: 11 March 2016 / Accepted: 25 May 2016 / Published online: 11 June 2016

Abstract The evolution of supercontinuum generation in chalcogenide suspended-core microstructured optical fibers is studied with regard to their exposure to the room atmosphere. We report the experimental proof of aging-induced supercontinuum generation drift in chalcogenide microstructured fibers. Mid-infrared supercontinuum covering the 2.5–5.5-μm spectral region is demonstrated in a fresh and 7-month-aged counterpart As_2S_3 fibers, by means of a home-built multistage oscillator power amplifier delivering 300 fs pulses at a repetition rate of 43 MHz in the 3.0–4.1-μm range. Numerical simulations based on the generalized nonlinear Schrödinger equation confirm the significant alteration of supercontinuum generation due to increasing fundamental OH and SH absorption bands.

Driven by the growing demand for sensing, medical, quality control, and other widespread applications, infrared (IR) supercontinuum light sources, particularly fibered ones, have known a great leap over the last few decades [1–11]. In this context, in practical terms, researchers have succeeded to overcome the opto-geometrical challenges by developing various special fiber geometries [4, 5, 7, 8, 12] and adopting innovative glass materials [13–15]. Among others, IR-transmitting chalcogenide-based suspended-core microstructured optical fibers (MOFs) have been extensively studied with encouraging prospects [16–21]. However, the most prominent achievements going beyond the limits induced by the previous geometry were recently obtained on similar chalcogenide-based step-index glass fibers [4, 6, 7, 9]. The usual design of MOFs consists in holes periodically arranged in the radial direction around a central core, and parallel to the axial direction. This configuration implies that the core of the fiber can be in contact with the ambient atmosphere which is naturally wet. It is precisely the presence of air holes that makes such fibers prone to contamination and subsequent degradation of their performance, particularly at OH- and SH-related wavelengths [22, 23]. When compared with standard step-index glass fibers, such MOFs are exposed to atmospheric conditions and external environment. This raises the question of the glass stability against aging in ambient atmosphere, as well the influence of fiber design on its efficiency for optical finalities. The last assumption of optical drift was extensively explored and unequivocally confirmed on the chalcogenide-based single-index glass fibers [24]. Nevertheless, all studies confirm that aging kinetics becomes more significantly pronounced on MOFs [22, 25, 26] as compared to single-index fibers [24]. In addition, within the MOF geometry, this kinetic drastically increases upon reducing the core size [27]. Under these circumstances, the presently presumed aging process seriously reduces the lifetime of the used MOF and severely compromises the SC generation efficiency [11, 25]. Overcoming such a drift is of major importance for implementation of supercontinuum sources in photonic devices for pertinent and long-term practical application.

Although the As–S MOFs are the most studied among numerous chalcogenide glass systems, their long-term

O. Mouawad and S. Kedenburg have contributed equally to this work.

✉ F. Smektala
frederic.smektala@u-bourgogne.fr

[1] Laboratoire Interdisciplinaire Carnot de Bourgogne, UMR 6303 CNRS-Université de Bourgogne Franche-Comté, 9 Av. Alain Savary, BP 47870, 21078 Dijon, France

[2] 4th Physics Institute and Research Center SCOPE, University of Stuttgart, 70550 Stuttgart, Germany

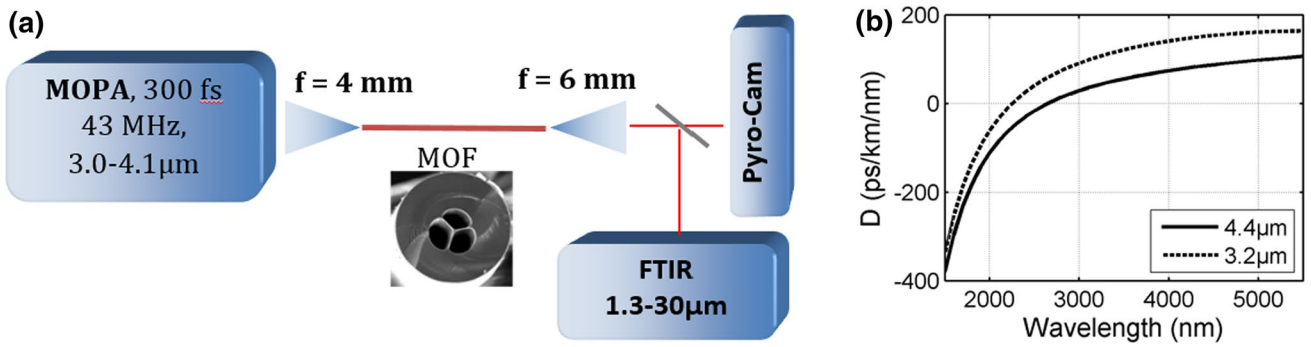

Fig. 1 **a** Experimental setup used for mid-IR SC generation in the suspended-core chalcogenide fiber (MOF). MOPA: optical parametric master oscillator power amplifier. *Inset*: cross-sectional image of our As_2S_3 suspended-core fiber captured by means of a scanning electron microscope. **b** Numerical dispersion curves of our As_2S_3 suspended-core fibers under study, with two different core sizes (4.4 and 3.2 µm)

efficiency regarding nonlinear optics applications, in particular SC generation, has been hardly investigated so far. The only study aiming to probe the impact of As–S MOF aging on the spectral broadening was reported by Mouawad et al. [25]. This work numerically investigated SC generation as a function of the fiber loss level using a previously validated numerical modeling. However, experiments supporting the previous findings remain to be demonstrated. To this aim, the present work experimentally confirms the detrimental aging of the MOF and directly related alterations of SC generation.

In this work, we report SC generation in a suspended-core As_2S_3 chalcogenide MOF. Two sets of supercontinuum generation measurements were performed. The first set was carried out on freshly drawn MOF samples, whereas for the second set, the same measurements were repeated with similar MOF samples after being stored under the crucial atmospheric conditions during 7 months. The variation of SC bandwidth was investigated by changing the pump wavelength, MOF length, and input power. With the aim of confirming the excessive aging upon decreasing the fiber core size (resp. increasing of surrounding holes size), MOFs with different core diameters (resp. various surrounding holes size) were probed. Experimental results were confirmed by numerical simulations based on the generalized nonlinear Schrödinger equation, and taking into account specific parameters to each sample.

Glass preforms for subsequent fiber drawing are cylindrical glass rods of 80 g in mass, 16 mm in diameter and approximately 80 mm in length. They were produced by the conventional melt-quenching technique of the adequate raw elements, in the appropriated stoichiometry, under vacuum in silica tubes, as detailed elsewhere [4]. In contrast to [4], elemental sulfur was adequately heated under dynamic vacuum at 350 °C, to remove the contaminating moisture. Preform designated for three-hole suspended-core MOF drawing was prepared by the mechanical drilling technique. Spectral losses of the used glass were measured on single-index fibers by means of a FTIR spectrometer and using cutback technique. Attenuation spectrum revealed an optical background of 2 dB/m and with additional losses of 1 dB/m and 8 dB/m at 2.9 µm and 4.0 µm (fundamental OH and SH absorption peaks), respectively. Note that we will also consider some linear losses above 5 µm (level similar to the SH peak) as already pointed out in Refs. [4, 28] for fibers made from extra-high-purity chalcogenide glass As_2S_3.

Figure 1 depicts the experimental setup used for mid-IR SC generation. A multistage oscillator power amplifier geometry was used following a similar approach as the one described in Refs. [29, 30]. The home-built laser source is tunable between 3.0 and 4.1 µm, with pulse duration of 300 fs, and a repetition rate of 43 MHz. After being separated from the signal residual by a short-pass filter, the incoupling pulses were focused by means of a 4-mm focal length IR objective (NA of 0.56) into the suspended-core As_2S_3 fiber, which in turn was fixed onto three-axis translation stage. This objective delivers up to 86–94 % depending on the wavelength of the laser radiation to the fiber. MOFs were cleaved by means of a scalpel blade, and quality of the interfaces was carefully checked under microscope before being characterized. An IR camera (Pyrocam 3, Spiricon) was used at the output end of the fiber to optimize the beam shape and to adjust the focal point, as well to ensure that light is exclusively guided into the MOF core. The generated SC was free-space-coupled and analyzed by means of a Fourier transform infrared spectrometer (Frontier FTIR spectrometer, PerkinElmer) operating in the 1.2–30-µm spectral range.

As stated above, the overall study in the present work is based on two sets of measurements on aged and fresh MOF segments. For each set, our experiments consist of three stages, aiming to probe the impact of the pump wavelength, the fiber length, as well as the input peak power on SC

generation, thus revealing the relationship between aging of the MOF and alterations of mid-IR SC generation.

1 Supercontinuum generation versus pump wavelength

First, we fixed the mean output power of the laser pump coupled into a defined fiber segment and tuned the central wavelength (λ_p) of the pulse spectrum. Figure 2a, c shows the experimental spectra recorded at the output of a 25-mm-long MOF segment for a fixed incident average power of 190 mW (4.4 nJ pulse energy) and pumping wavelengths ranging from 3.0 to 4.1 µm. The output supercontinua were generated with average powers varying between ~20 and ~30 mW, in aged and fresh MOF segments with a 4.4-µm core diameter, respectively. Here, without taking into account the Fresnel losses (17 % per facet for As_2S_3), the measured output power was ~11 and ~15 % of the incident power, whatever the input wavelength. This is mainly attributed to the low coupling efficiency due to the discrepancy between mode field diameters of the optical parametric amplifier idler and the MOF, which are >5.0 and 4.4 µm, respectively.

The corresponding zero-dispersion wavelength (ZDW) of our MOF segments was estimated about 2.65 µm from vector mode calculations based on the fiber geometry derived from the SEM image of their cross section, as shown in Fig. 2b. Nonlinear spectral broadening that occurs in the present pumping condition of strong anomalous dispersion (about 45–75 ps/km/nm) is then strongly related to soliton dynamics toward the long-wavelength edge, as shown in Fig. 2a. We notice that upon tuning upward the pump wavelength, both short- and long-wavelength edges of the SC spectra were shifted in the mid-IR region. After propagating in the fresh chalcogenide MOF, the spectrum was strongly broadened and covers almost 2000 nm over 30-dB dynamic range. However, the spectral bandwidth crucially decreased to below 1200 nm, on the counterpart aged specimen. This confirms the typical nonlinear behavior in a MOF which was influenced by the deleterious aging phenomena [22, 25]. For aged MOF, additional optical losses which have grown over the exposure period severally reduced the MOF transmission efficiency and explain the collapse of the output power as compared to the fresh sample. This behavior was unequivocally confirmed on the aged MOF after several attempts to pump the sample around 3 µm. During these experiments, despite the repeated trials, output signal was not detected, or even imaged by the IR-Pyro-camera. This is due to the excessive OH absorption occurring around 3 µm, resulting from the advanced aging process within the MOF. Note that we observe in Fig. 2a characteristic dip, which randomly

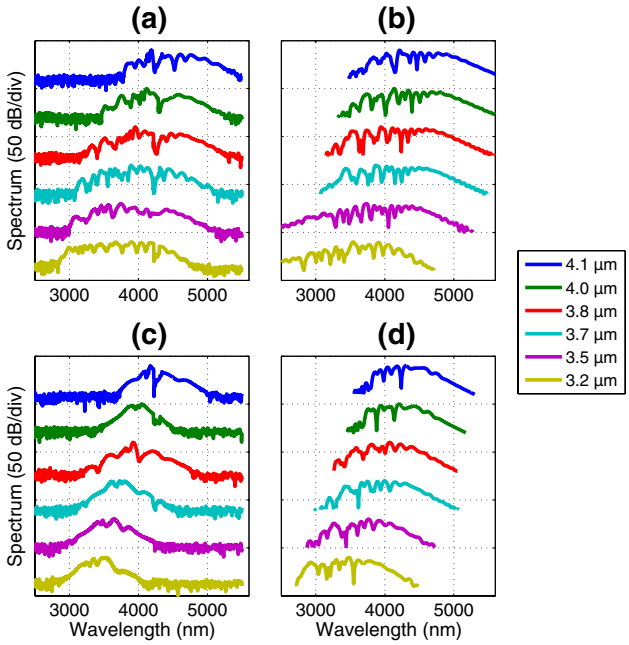

Fig. 2 **a**, **c** Experimental and **b**, **d** numerical SC spectra for various pump wavelengths from 3.2 to 4.1 µm in 25-mm-long (**a**, **b**) fresh and (**c**, **d**) 7-months-aged As_2S_3 samples. For sake of clarity, each spectrum is displaced vertically by 40 dB, and numerical results are shown over 30-dB dynamic range

appears at 4.3 µm and is attributed to atmospheric absorption mainly caused by CO_2.

A detailed analysis based on numerical simulations was performed to elucidate the strong limitations imposed in the nonlinear dynamics of SC generation. Numerical results are obtained through the split-step Fourier-based solving of the generalized nonlinear Schrödinger equation (for single mode and single polarization) [31] taking into account the full dispersion curve from mode calculations (see Fig. 2b), measured fiber losses as well as self-steepening and analytical model of the Raman gain spectrum. For the Raman response function, we used an intermediate-broadening model using convolutions of Lorentzians and Gaussians adapted from spontaneous Raman scattering spectra and estimated Raman gain coefficient of our As_2S_3 glass system [19, 32, 33]. The nonlinear index is $n_2 \sim 2.8 \times 10^{-18}$ m^2/W [34], which gives a nonlinear Kerr coefficient $\gamma \sim 0.35$ 1/(W*m) in the wavelength range under study. This led to nonlinear length (L_{NL}) estimated around 1 mm at the considered input peak power; the injected pulse corresponds to a low soliton number $N < 20$ due to the strong anomalous dispersion regime [31]. Therefore, the SC spectra are characterized by the usual self-phase modulation process followed by soliton fission in the first centimeter of propagation. Subsequent propagation is then driven by Raman soliton self-frequency shift toward longer wavelengths. As Fig. 2b shows, when taking only into account the loss

level experimentally measured for the single-index fiber, the simulated SC spectra are in good agreement with those experimentally obtained with the fresh MOF. However, discrepancies became more significant when the experimental spectra of the aged MOF (see Fig. 2d) were considered. The best matching between simulations and experiments was achieved upon taken into account extra losses mainly for the optical background about 20 dB/m, at 2.9 and 4.0 μm (about 75 dB/m for OH and SH absorption peaks, respectively) and for wavelengths above 5 μm, in a similar way to what had been previously raised in [4, 22, 25, 28]. These results confirm beyond any doubt the previously presumed glass aging over time upon exposure to atmosphere [22] and their inherent deleterious impact on the nonlinear effects at the origin of the spectral broadening [25].

Throughout this work, in spite of the convenient qualitative fit between the simulation and experience, a slight mismatch remains present. This might be related to the deviation of the simulated dispersion profile that would affect the shape and range of the simulated SC. In addition, the drift of the measured coupling efficiency between the focal objective and the tested MOF would cause the change in the peak powers really employed. These experimental works that involve mid-infrared coupling (collection) in (from) small fiber cores over such a large range of wavelengths are quite challenging.

2 Supercontinuum generation versus fiber length

Here, we fixed the central wavelength of the pump at 3.5 μm and the incident power at 270 mW (estimated coupled power ~35–40 mW), and we changed the length of the probed fibers. Figure 3 reports the corresponding SC spectra obtained for different lengths ranging from 25 to 110 mm. It should be noted that during this study, the coupling efficiencies were similar to those reported above. The spectral broadening in the fresh MOFs (Fig. 3a) appears weakly affected by the fiber length, thus evidencing the low fiber losses. For all tested lengths, the output spectrum covered almost the same spectral range. Nevertheless, the largest bandwidth was achieved with the 45-mm-long segment due to possible losses beyond 5 μm. Besides the significant loss of broadening and flatness, SC generated in aged counterpart MOFs also exhibits a strong dependence on the fiber length (see Fig. 3c). The present observation confirmed the crucial aging and its inherent deleterious impact on nonlinear dynamics, in the aged fiber as compared to the fresh one. In both cases, the broadest SC is obtained for very short segments of MOFs, but for the aged fiber, the limitation comes from the SH absorption band around

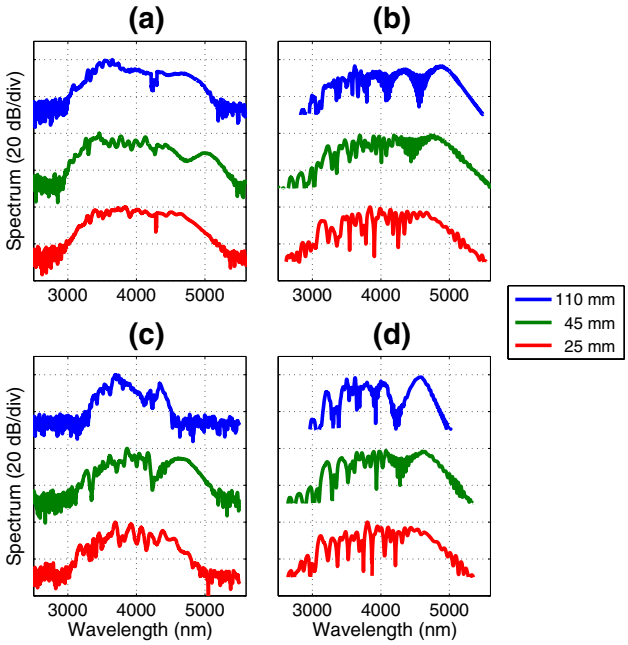

Fig. 3 **a**, **c** Experimental and **b**, **d** numerical SC spectra obtained by pumping at 3.5 μm in various fiber lengths of (**a**, **b**) fresh and (**c**, **d**) aged As_2S_3 samples. For sake of clarity, each spectrum is displaced vertically by 40 dB, and numerical results are shown over 30-dB dynamic range

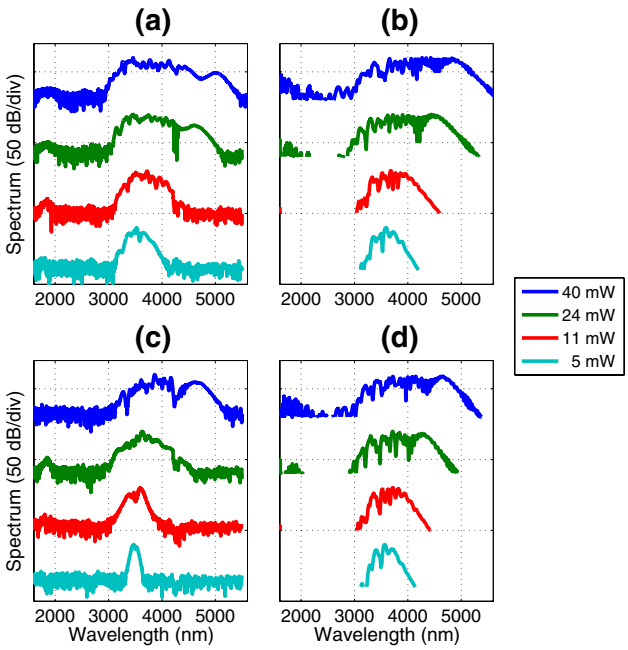

Fig. 4 **a**, **c** Experimental and **b**, **d** numerical SC spectra obtained for different incident powers at 3.5 μm in 45-mm-long segments of (**a**, **b**) fresh and (**c**, **d**) aged As_2S_3 fibers. For sake of clarity, each spectrum is displaced vertically by 40 dB, and numerical results are shown over 30-dB dynamic range

4.1 μm and from losses around 5 μm [4, 28]. This analysis of experiments is confirmed by our numerical simulations shown in Fig. 3b, d. As stated above, under the presumed pumping regime, the spectral broadening effects in this regime are dominated by soliton-related dynamics. In the fresh fiber, the Raman soliton self-frequency shift toward longer wavelengths is very efficient since there is no significant absorption around 4.1 μm. However, for the 110-mm-long segment, our experimental SC does not extend beyond 5.2 μm in the fresh fiber, and the spectral bandwidth even decreases in the aged fiber segment and restrains to 4.5 μm. Even if extra losses between 5 and 6 μm resulting from the glass aging were considered in the simulations (i.e., about 75 dB/m), some accurate and direct measurements of those losses are required to better fit the experiments.

3 Supercontinuum generation versus input power

After selecting the optimal sample length (45 mm) and pumping wavelength (3.5 μm), we investigate the influence of input power on the spectral broadening. Figure 4a, c shows the dependence of the SC spectral width on the estimated input average power. Both width and flatness of the generated SC evolve in a similar manner, whatever the considered sample. A continuous flat spectrum extends from 2.9 to 5.5 μm results in the fresh fiber for the maximum power, whereas it remains narrower (3–5.1 μm) on the aged counterpart fiber. Corresponding numerical simulations are given in Fig. 4b, d; a good agreement is obtained for both fresh and aged samples. Again the previous aging-induced losses were taken into account in the case of aged MOF. This provides additional evidence of the previously presumed [22, 25] time evolution of deleterious extrinsic absorption bands within the glass fibers upon exposure to room atmosphere. It is clear that significant differences appear between SC spectra recorded in fresh and aged MOFs when the input power reaches 24 mW. It mainly occurs when spectral broadening extends beyond 4.1 μm (i.e., typical wavelength feature of SH extrinsic absorption) and approaches 5 μm. This provides again a proof of the dynamic time evolution of glass optical properties, in particular, the impact of atmospheric moisture through interaction with the glass network, as previously reported in [23].

It is worth mentioning that Fig. 4 also reveals the presence of a spectral bump just below 2 μm and continuously growing upon increasing the power. It was successfully reproduced in numerical results on both probed fiber samples. Due to the large detuning of the pump wavelength from the ZDW, during the initial pulse breaking, the initial pulse and subsequent generated solitons emit some dispersive wave radiations with reduced energy in the normal dispersion regime [31]. Furthermore, the dispersive

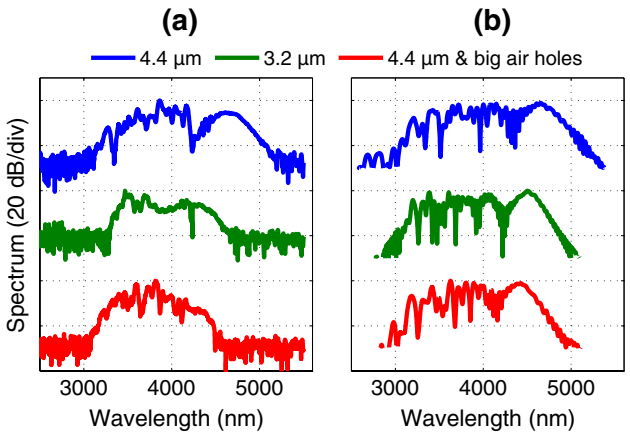

Fig. 5 **a** Experimental and **b** numerical SC spectra obtained by pumping at 3.5 μm various core-size (or hole-size) aged fibers, the sample length is 45 mm. For sake of clarity, each spectrum is displaced vertically by 40 dB, and numerical results are shown over 30-dB dynamic range

wave was very difficult to observe experimentally in that wavelength range, so we did not present them in previous figures. Consequently, we can wisely consider that the dip systematically occurring between 2 and 3 μm is inherent to the nonlinear dynamics which govern the spectral broadening.

4 Supercontinuum generation versus core and holes size

The holes running along the length of the MOFs are essential for their performance. They are advantageous for light guidance (confinement) and scaling down the ZDW for efficient nonlinear dynamics. In general, for SC generation purposes, small-core chalcogenide-based MOFs are conceived. Nevertheless, previous work performed on silica MOFs proved that optical degradation for the smallest core MOF occurs more rapidly than that for bigger cores [27]. Admitting that chalcogenide glasses are more prone to degradation than silica glass, efficiency of nonlinear dynamics is expected to severely decline, and subsequently SC bandwidth sharply decreases. With the aim to elucidate the previous hypothesis, SC generation measurements were taken in two aged MOFs with different core diameters, 4.4 and 3 μm, respectively. Note that the ZDW of our 3-μm core MOF was estimated close to 2.25 μm. The comparison of SC spectra for similar input power is given in Fig. 5, and it clearly demonstrates a spectral narrowing and flatness deterioration over time more pronounced within the smaller core MOF. These results were confirmed by numerical simulations that use extra losses in the smaller core about two times the above levels of the larger core. Such values are

again in agreement with what had been previously used in Refs. [4, 22, 25] for a 3.2-μm core MOF.

In a previous work, Mouawad et al. [23] confirmed that MOF aging is due to atmospheric moisture diffusion in the holes of the fiber. According to diffusion laws, one would expect that with bigger holes water vapor is liable to enter faster into the fiber structure to subsequently contaminate the guiding core. With aim to prove this behavior, two MOFs of the same core diameter and different air-filling fraction (A) were tested. The "A" was calculated from the SEM images. For the regular MOF, A = 0.11; however, this value increases to 0.25 on the inflated one. Figure 5 gathers the spectra recorded on both probed MOF specimen and unequivocally confirms the presumed effect. Numerical simulations confirmed this behavior by using the same aging-induced losses than in the 3-μm core MOF.

In front of this crucial effect drastically limiting the fibers efficiency, innovative preventive solutions become an assist. From this perspective, a first strategy based on holes proofing was previously suggested and confirmed in [22]. In addition, manipulating the suspended-core fibers under controlled dry atmosphere is an efficient alternative technique. Another strategy, which consists in filling the holes with other glass materials, such as in filled holes hybrid suspended-core fibers, allows to avoid such a drastic phenomenon.

Our extensive study of mid-infrared supercontinuum generation in fresh and 7-months-aged As_2S_3 microstructured optical fibers clearly confirm the significant alteration of supercontinuum generation due to increasing background losses and growing fundamental OH and SH absorption bands. The dynamic time evolution of glass optical properties, in particular, the detrimental impact of atmospheric moisture through interaction with the glass network, strongly reduces the nonlinear spectral broadening in such fibers. We report the accelerated degradation of supercontinuum generation for smaller core microstructured optical fibers and for microstructured fibers with big air holes, the atmospheric moisture diffusion toward the fiber core being facilitated in such cases. This has implications for the treatment and storage of optical fiber prior to nonlinear optics experiments and highlights the need to step-index optical fibers as part of the fiber protection procedure. Given the recent improvements of femtosecond laser sources toward long mid-infrared wavelengths, step-index chalcogenide fibers appear as a more robust solution for developing mid-infrared supercontinuum sources for long-term applications with non-controlled atmosphere [35].

Acknowledgments We acknowledge the financial support from the Conseil Régional de Bourgogne and the FEDER European program through the Photcom PARI program. This project has been performed in cooperation with the Labex Action program (contract ANR-11-LABX-0001-01).

References

1. M.L. Naudeau, R.J. Law, T.S. Luk, T.R. Nelson, S.M. Cameron, J.V. Rudd, Opt. Express **14**, 6194–6200 (2006)
2. R.R. Gattass, L.B. Shaw, V.Q. Nguyen, P.C. Pureza, I.D. Aggarwal, J.S. Sanghera, Opt. Fiber Technol. **18**, 345–348 (2012)
3. D.D. Hudson, M. Baudisch, D. Werdehausen, B.J. Eggleton, J. Biegert, Opt. Lett. **39**, 5752–5755 (2014)
4. O. Mouawad, J. Picot-Clémente, F. Amrani, C. Strutynski, J. Fatome, B. Kibler, F. Désévédavy, G. Gadret, J.C. Jules, D. Deng, Y. Ohishi, F. Smektala, Opt. Lett. **39**, 2684–2687 (2014)
5. C.R. Petersen, U. Moller, I. Kubat, B. Zhou, S. Dupont, J. Ramsay, T. Benson, S. Sujecki, N. Abdel-Moneim, Z. Tang, D. Furniss, A. Seddon, O. Bang, Nat. Photonics **8**, 830–834 (2014)
6. F. Théberge, N. Thiré, J.-F. Daigle, P. Mathieu, B.E. Schmidt, Y. Messaddeq, R. Vallée, F. Légaré, Opt. Lett. **39**, 6474–6477 (2014)
7. U. Møller, Y. Yu, I. Kubat, C.R. Petersen, X. Gai, L. Brilland, D. Méchin, C. Caillaud, J. Troles, B. Luther-Davies, O. Bang, Opt. Express **23**, 3282–3291 (2015)
8. Y. Yu, B. Zhang, X. Gai, C. Zhai, S. Qi, W. Guo, Z. Yang, R. Wang, D.-Y. Choi, S. Madden, B. Luther-Davies, Opt. Lett. **40**, 1081–1084 (2015)
9. T.M. Monro, H. Ebendorff-Heidepriem, Annu. Rev. Mater. Res. **36**, 467–495 (2006)
10. W. Gao, Z. Duan, K. Asano, T. Cheng, D. Deng, M. Matsumoto, T. Misumi, T. Suzuki, Y. Ohishi, J. Appl. Phys B **116**, 847–853 (2014)
11. I. Savelli, O. Mouawad, J. Fatome, B. Kibler, F. Désévédavy, G. Gadret, J.C. Jules, P.Y. Bony, H. Kawashima, W. Gao, T. Kohoutek, T. Suzuki, Y. Ohishi, F. Smektala, Opt. Express **20**, 27083–27093 (2012)
12. Y. Yu, X. Gai, P. Ma, D.-Y. Choi, Z. Yang, R. Wang, S. Debbarma, S.J. Madden, B. Luther-Davies, Laser Photon. Rev. **8**, 792–798 (2014)
13. A. Al-kadry, C. Baker, M. El Amraoui, Y. Messaddeq, M. Rochette, Opt. Lett. **38**, 1185–1187 (2013)
14. S. Shabahang, G. Tao, J.J. Kaufman, A.F. Abouraddy, J. Opt. Soc. Am. B **30**, 2498–2506 (2013)
15. C.W. Rudy, A. Marandi, K.L. Vodopyanov, R.L. Byer, Opt. Lett. **38**, 2865–2868 (2013)
16. V. Kokorina, *Glasses for Infrared Optics* (The CRC Press, Boca Raton, 1996)
17. Y.D. West, T. Schweizer, D.J. Brady, D.W. Hewak, Fiber Integr. Opt. J. **19**, 229–250 (2000)
18. A.A. Wilhelm, C. Boussard-Plédel, Q. Coulombier, J. Lucas, B. Bureau, P. Lucas, Adv. Mater. **19**, 3796–3800 (2007)
19. J.S. Sanghera, L.B. Shaw, I.D. Aggarwal, IEEE J. Sel. Top. Quantum Electron. **15**, 114–119 (2009)
20. D.W. Hewak, D. Brady, R.J. Curry, G. Elliott, C.C. Huang, M. Hughes, K. Knight, A. Mairaj, M.N. Petrovich, R.E. Simpson, in *Chalcogenide Glasses for Photonics Device Applications* (Research Signpost, 2010)
21. S. Cui, C. Boussard-Plédel, J. Lucas, B. Bureau, Opt. Express **22**, 21253–21262 (2014)
22. O. Mouawad, C. Strutynski, J. Picot-Clémente, F. Désévédavy, G. Gadret, J.C. Jules, F. Smektala, Opt. Mater. Express **4**, 2190–2203 (2014)
23. O. Mouawad, P. Vitry, C. Strutynski, J. Picot-Clémente, F. Désévédavy, G. Gadret, J.C. Jules, E. Lesniewska, F. Smektala, Opt. Mater. **44**, 25–32 (2015)
24. M.F. Churbanov, V.S. Shiryaev, V.V. Gerasimenko, A.A. Pushkin, I.V. Skripachev, G.E. Snopatin, V.G. Plotnichenko, Inorg. Mater. **38**, 1063–1068 (2002)

25. O. Mouawad, F. Amrani, B. Kibler, J. Picot-Clémente, C. Strutynski, J. Fatome, F. Désévédavy, G. Gadret, J.C. Jules, O. Heintz, E. Lesniewska, F. Smektala, Opt. Express **22**, 23912–23919 (2014)
26. P. Toupin, L. Brilland, D. Mechin, J. Adam, J. Troles, J. Lightwave Technol. **32**, 2428–2432 (2014)
27. I.G. Sanchez, Fabrication and Applications of low OH Photonic Crystal Fibers. in *Department of Physics* (University of Bath, Bath, 2012), p. 131
28. G.E. Snopatin, V.S. Shiryaev, V.G. Plotnichenko, E.M. Dianov, M.F. Churbanov, Inorg. Mater. **45**, 1439–1460 (2009)
29. T. Steinle, F. Neubrech, A. Steinmann, X. Yin, H. Giessen, Opt. Express **23**, 11105–11113 (2015)
30. F. Mörz, T. Steinle, A. Steinmann, H. Giessen, Opt. Express **23**, 23960–23967 (2015)
31. J.M. Dudley, J.R. Taylor, *Supercontinuum Generation in Optical Fibers* (Cambridge University, Cambridge, 2010)
32. R.J. Kobliska, S.A. Solin, Phys. Rev. B **8**, 756–768 (1973)
33. R. Stegeman, G. Stegeman, P. Delfyett Jr., L. Petit, N. Carlie, K. Richardson, M. Couzi, Opt. Express **14**, 11702–11708 (2006)
34. V.G. Ta'eed, N.J. Baker, L. Fu, K. Finsterbusch, M.R.E. Lamont, D.J. Moss, H.C. Nguyen, B.J. Eggleton, D.Y. Choi, S. Madden, B. Luther-Davies, Opt. Express **15**, 9205–9221 (2007)
35. S. Kedenburg, T. Steinle, F. Morz, A. Steinmann, H. Giessen, Opt. Lett. **40**, 2668–2671 (2015)